Shoulder motion during tennis serve: dynamic and radiological evaluation based on motion capture and magnetic resonance imaging

Caecilia Charbonnier[a,*], Sylvain Chagué[a], Frank C. Kolo[b], Alexandre Lädermann[c,d]

[a] *Artanim Foundation, Medical Research Department, Geneva, Switzerland*
[b] *Rive Droite Radiology Center, Geneva, Switzerland*
[c] *Division of Orthopaedics and Trauma Surgery, La Tour Hospital, Geneva, Switzerland*
[d] *Faculty of Medicine, University of Geneva, Geneva, Switzerland*

* Corresponding author:
C. Charbonnier
Medical Research Department
Artanim Foundation
41b route des Jeunes
1227 Carouge - Switzerland
Tel.: +41 (0)22 596 45 40
Fax: +41 (0)22 320 07 76
Email: caecilia.charbonnier@artanim.ch

Abstract

Purpose: Rotator cuff and labral lesions in tennis players could be related to posterosuperior internal impingement or subacromial impingement during tennis serve. However, it is unknown which of these impingements are responsible for the lesions found in the tennis player's shoulder. Moreover, there is a lack of validated non-invasive methods and dynamic studies to ascertain impingement during motion.

Methods: Ten intermediate or ex-professional tennis players were motion captured with an optical tracking system while performing tennis serves. The resulting computed motions were applied to patient-specific shoulder joints 3D models based on Magnetic Resonance Imaging (MRI) data. During motion simulation, impingements were detected and located using computer-assisted techniques. An MRI examination was also performed to evaluate the prevalence of shoulder lesions and to determine their relevance with the simulation findings.

Results: Simulation showed that internal impingement was frequently observed compared to subacromial impingement when serving. The computed zones of internal impingement were mainly located in the posterosuperior or superior region of the glenoid. These findings were relevant with respect to radiologically diagnosed damaged zones in the rotator cuff and glenoid labrum.

Conclusions: Tennis players presented frequent radiographic signs of structural lesions which seem to be mainly related to posterosuperior internal impingement due to repetitive abnormal motion contacts. The present study indicates that the practice of tennis serve could lead with time to cartilage/tendon hyper compression, which could be damageable for the glenohumeral joint.

Keywords: Shoulder kinematics; Motion capture; MRI; 3D Simulation; Impingement; Tennis

1. Introduction

Impingement of the shoulder is a common cause of shoulder pain in tennis players due to repetitive overhead arm movements [10, 20, 27]. Impingement occurs during tennis serves leading with time to rotator cuff and/or labral tears [1, 10, 20, 27]. Two different impingements have been described: 1) the posterosuperior internal impingement [35] of the rotator cuff tendons (supraspinatus/ infraspinatus) and glenoid labrum between the greater tuberosity of the humeral head and the posterosuperior aspect of the glenoid when the arm is in extreme abduction, extension and external rotation [12] during the late cocking stage of the serve; 2) the subacromial impingement of the rotator cuff between the anterior acromion [25] or lateral acromion [26] and the superior humeral head.

To our knowledge, impingements during tennis serve have never been dynamically evaluated in-vivo. It is therefore unknown which of the aforementioned impingements are responsible for the lesions found in the tennis player's shoulder. According to the impingement theory, shoulder damage occurs at the zone of impingement but the concurrence of the actual impingement zone and resulting joint damage in the same patient has not yet been confirmed. Moreover, there is a lack of validated non-invasive methods to ascertain impingement during motion. Existing imaging methods only include a static interpretation of the joint damage (e.g., computed tomography (CT), magnetic resonance imaging (MRI)), while dynamic imaging protocols (e.g., MRI, fluoroscopy) are affected by technical limitations (e.g., confined area of measurement, low acquisition speed).

Motion capture systems using skin-mounted markers provide a good solution to non-invasively record large ranges of motion during high velocity movements, such as in tennis strokes. However, drawbacks are related to soft tissue artifacts (STA) affecting kinematic estimation [17, 37], in particular precise joint translation that is crucial to assess glenohumeral impingement. In previous work [6], we have demonstrated that this issue could be effectively tackled. Combined with computer-assisted techniques and anatomical models obtained from medical images, we believe that motion capture can offer novel insights into the analysis and comprehension of shoulder impingement.

As the serve is among the most important strokes in tennis, it has been the subject of significant biomechanical interest. Motion capture systems were used to investigate the kinematics and kinetics of lower and upper limb joint motion [11, 28, 38, 39] as a function of serve type [28], body mass index [39], and racket type [11, 38]. Attention has also been afforded to the interaction of the ball and racket during the serve [30, 38]. Despite these advancements, recent research has not devoted specific attention to the direct consequences of the practice of tennis serve on the internal joint structures. This study intended to be a step in this direction.

In this paper, we present a methodology to perform functional simulations of patient-specific shoulder joints during extreme and complex positions, as well as the results of a study conducted with tennis players. The purpose of this research was to visualize and simulate in 3D shoulder motion during tennis serve and to detect and locate potential impingement during their practice, using optical motion capture and computer-assisted techniques. In addition, this study aimed at evaluating the prevalence of shoulder lesions in this group of tennis players based on MRI and at determining their relevance with the simulation findings.

2. Materials and Methods

2.1. Subjects

Ten intermediate or ex-professional tennis players (one female, nine males) volunteered for the study. The mean age, weight, height and body mass index of the ten volunteers were 39.7 years, 76.7 kg, 180.2 cm and 23.5 kg/m^2, respectively. Exclusion criteria were reported previous shoulder injuries, shoulder surgery or contraindications for MRI.

At the time of the examination, two subjects presented shoulder pain and nine previously suffered from the shoulder at other moment of their career. All subjects had a clinically functional rotator cuff.

The dominant arm was used throughout testing. This was the right arm for all participants, except one who was left hand dominant. Institutional ethical approval and informed consent were obtained prior to data collection.

2.2. MRI and three-dimensional reconstruction

All volunteers underwent a MR shoulder arthrography. The MRI examinations were conducted after a fluoroscopically guided arthrography with a contrast agent and with an anterior approach. MRI was performed with a 1.5 T HDxT system (General Electric Healthcare, Milwaukee WI, USA). A dedicated shoulder surface coil was used. The following MRI sequences were acquired: 1) a sagittal T1 weighted fast spin echo sequence (section thickness 3.5 mm; gap 0.5 mm; TR/TE ms 380/11), 2) a coronal T2 weighted fast spin echo sequence with fat saturation (section thickness 4 mm; gap 0.5 mm; TR/TE ms 1920/101.6), 3) a sagittal T2 weighted fast spin echo sequence with fat saturation (section thickness 3.5 mm; gap 0.5 mm; TR/TE ms 5680/103.6), 4) a coronal T1 weighted fast spin echo sequence with fat saturation (section thickness 4 mm; gap 0.5 mm; TR/TE ms 320/13), 5) an axial T1 weighted fast spin echo sequence with fat saturation (section thickness 4 mm; gap 0.5 mm; TR/TE ms 640/26.8), 6) an axial Cosmic® 3D fast gradient echo sequence with fat saturation (section thickness 1.8 mm; no gaps; TR/TE ms 6.1/3.0), 7) an axial Cosmic® 3D fast gradient echo sequence (section thickness 4 mm; no gaps; TR/TE ms 5.7/2.8), and 8) an axial Lava® 3D fast gradient echo sequence (section thickness 5.2 mm; no gaps; TR/TE ms 3.7/1.7).

Two musculoskeletal radiologists, blinded to the clinical evaluation, assessed independently all MRI arthrograms for shoulder pathology. The rotator cuff abnormalities [33], the labral lesions [36] and the bony changes [24] were reviewed. Rotator cuff lesions were classified as partial articular surface tendon avulsion lesion, bursal-sided partial thickness tear, interstitial tear, or complete tear (Fig. 1). The glenoid labrum was considered as normal, degenerated (abnormal signal intensity), torn (abnormal linear intensity extending to the glenoid surface), detached (abnormal linear intensity coursing at the interface between bone and labrum at the level or posterior to the attachment of biceps tendon) or as ossification of the labrum (continuity of the labrum with glenoid bone marrow). The absence or presence of bony changes such as Bankart lesions [2] or intra-osseous cysts was reported.

The 3D MR images were manually segmented by one of the musculoskeletal radiologist (FCK) and a virtual 3D model of the shoulder complex was reconstructed using Mimics software (Materialize NV, Leuven, Belgium). For each tennis player, patient-specific 3D

models of the shoulder bones (humerus, scapula, clavicle and sternum), cartilage surfaces and labrum were obtained.

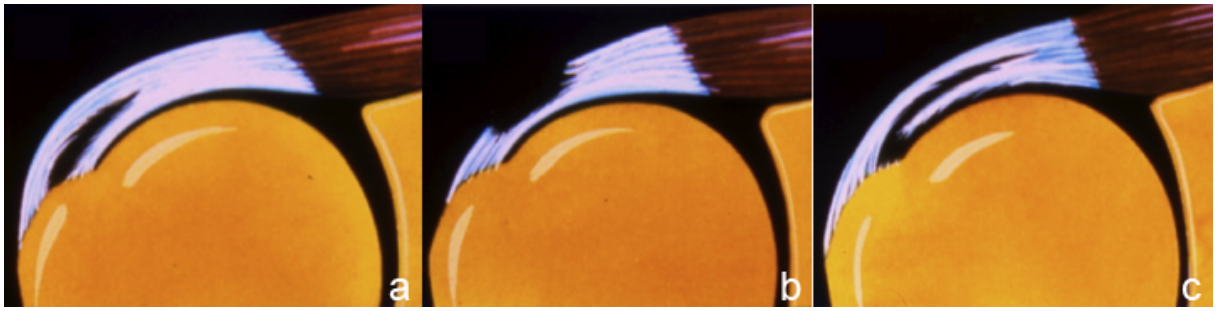

Fig. 1 a) Interstitial tear, b) bursal-sided partial thickness tear, c) partial articular supraspinatus tendon avulsion (PASTA) lesion.

To compute joint motion, local coordinate systems were established based on the definitions suggested by the International Society of Biomechanics [40] to represent the thorax, clavicle, scapula and humerus segments. They were created using anatomical landmarks identified on the reconstructed bone models and MR images. The glenohumeral joint center was calculated using a sphere fitting method [32].

2.3. Motion recording

The tennis players participated to a motion capture session. They were equipped with a dedicated shoulder markers protocol [6] (Fig. 2), including 69 spherical retroreflective markers placed directly onto the skin using double sided adhesive tape. The setup included 4 markers (Ø 14 mm) on the thorax (sternal notch, xyphoid process, C7 and T8 vertebra), 4 markers (Ø 6.5 mm) on the clavicle, 4 markers (Ø 14 mm) on the upper arm – two placed on the lateral and medial epicondyles and two as far as possible from the deltoid – and 57 markers on the scapula (1x Ø 14 mm on the acromion and a 7x8 grid of Ø 6.5 mm). Additional markers were distributed over the body (non-dominant arm and legs) to provide a global visualization of the motion.

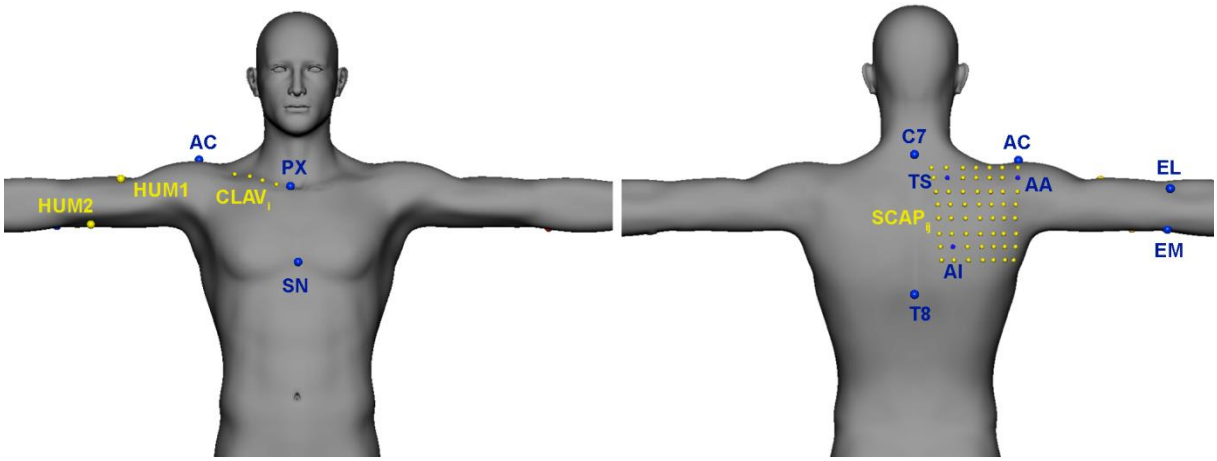

Fig. 2 Markers placement including markers placed on anatomical landmarks (blue) and technical markers (yellow). PX = xyphoid process, SN = sternal notch, AC = acromion, TS = trigonum spinae, AA = angulus acromialis, AI = angulus inferior, EL = lateral epicondyle, EM = medial epicondyle.

After appropriate warm-up, participants performed three trials of the following variants of tennis serve: flat serve, when the ball is hit down and through with little to no spin; and kick serve, when the ball is hit with an upward motion, imparting top-spin on the ball. Motion was recorded using a Vicon MXT40S motion capture system (Vicon, Oxford Metrics, UK) consisting of 24 cameras sampling at 240 Hz. The same investigators (CC, SC) attached all markers and performed all measurements.

2.4. Kinematics modeling

Shoulder kinematics was computed from the recorded markers' trajectories. Measuring shoulder motion using skin-mounted markers is a challenging task. The first issue is related to the accuracy of the measurements which is prone to error due to the non-rigid movement of the soft tissue interface between the skin markers and the underlying bone, commonly referred to as soft tissue artifact [17]. In the upper extremity, the scapula is particularly affected [37]. The second issue is related to the ability to estimate both shoulder joint rotation and translation using an external measurement system – information about joint translation is crucial to properly assess glenohumeral impingement.

To address these two issues, we used a previously developed and validated biomechanical model based on a patient-specific kinematic chain consisting of four rigid bodies (thorax, clavicle, scapula and humerus) using the tennis player's shoulder 3D models reconstructed from their MRI data. To register internal anatomical structures to the marker cluster frames, a calibration was performed based on a standard CAST (Calibrated Anatomical System Technique) protocol [31]. The optimal pose of the kinematic chain was then obtained by using a global optimization algorithm (to minimize STA error globally [29]) with loose constraints on joint translations. More details about the model and its validation can be found in [6]. The accuracy of the model for glenohumeral orientation was within 4° for each anatomical plane and within 3 mm for glenohumeral translation. Moreover, previous results showed that the translation patterns computed with the model were in good agreement with related works [21, 22].

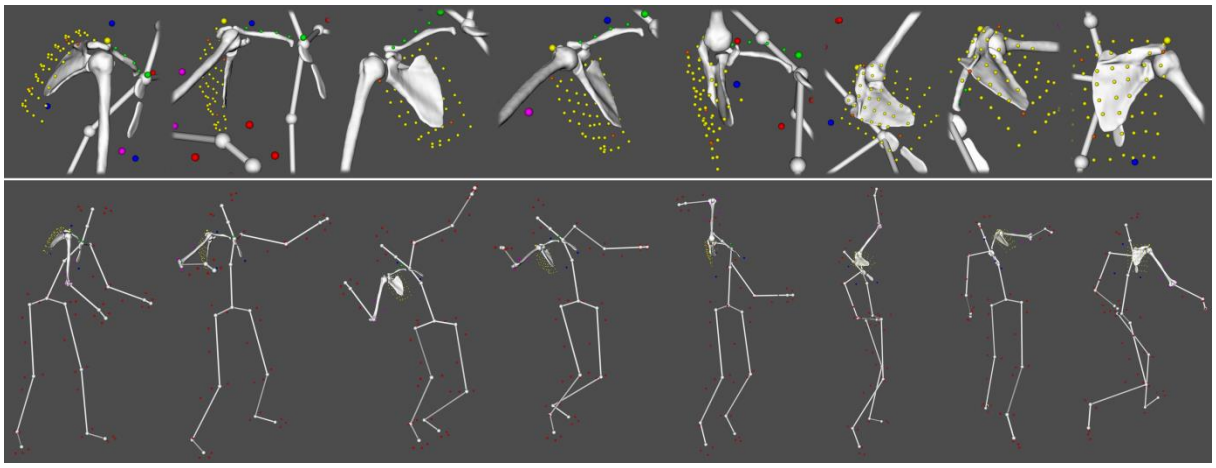

Fig. 3 Kinematic animation of the shoulder (here the right shoulder joints) during flat serve. Top images show a zoom in the shoulder for each position. Position 4 is commonly known as the cocking stage.

As a result, the motion of the tennis player's shoulder 3D models could be visualized at each point of the movement. Figure 3 shows an example of computed bone poses during

tennis serve. A ball and stick representation of the overall skeleton was also added to improve the analysis and visualization of the motion.

2.5. Impingement detection

During motion simulation, internal and subacromial impingements were evaluated at the critical position – the late cocking stage of the serve (see Fig. 3). For internal impingement, a collision detection algorithm [4, 5] was used to virtually locate contacts between the humeral cartilage, the glenoid cartilage and the glenoid labrum. Moreover, the surface-to-surface distance (i.e., penetration depth) was computed in order to estimate the overall impingement. This distance represented the topographic extent of the cartilage or labral compression and was reported in millimeter.

To document areas of increased compression, the penetration depth distribution on the surface of the cartilages and labrum was represented using a color scale (Fig. 4a). The blue color was assigned when no collision was detected (penetration depth = 0), while other colors showed the compression zone. The red color denoted the area with the highest compression (penetration depth = max).

To describe and report the exact location of the impingement zone, the glenoid was divided into eight sectors (position 1, anterior; position 2, anterosuperior; position 3, superior; position 4, posterosuperior; position 5, posterior; position 6, posteroinferior; position 7, inferior; position 8, anteroinferior), as depicted in Figure 4b. The impingement zones were hence assigned numbers correlating with their position.

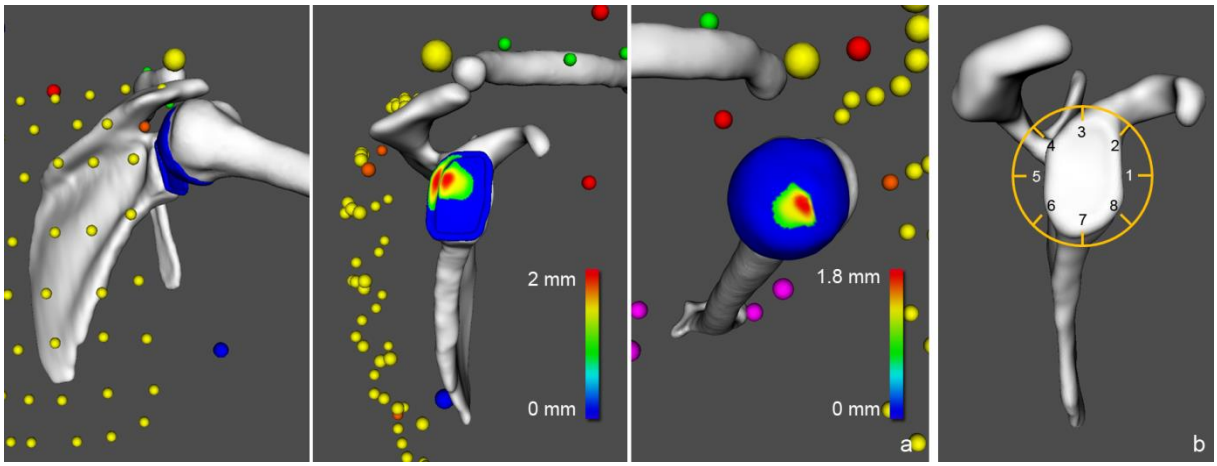

Fig. 4 a) Visualization of the contact zone during motion (posterior, lateral and medial views). The colors represent the penetration depth distribution: the blue color is assigned when no collision is detected (penetration depth = 0), while other colors show the compression zone. The red color denotes the area with the highest compression (penetration depth = max). Note: the humerus and humeral cartilage, respectively the scapula, glenoid cartilage and labrum are not shown in the lateral and medial views for clarity. b) Glenoid divided into eight sectors (position 1, anterior; position 2, anterosuperior; position 3, superior; position 4, posterosuperior; position 5, posterior; position 6, posteroinferior; position 7, inferior; position 8, anteroinferior) to report the location of the impingement zone.

For subacromial impingement, the minimum humero-acromial distance that is typically used for the evaluation of such impingement was measured [8, 14, 34]. This distance was calculated in 3D based on the simulated bones models positions and was reported in millimeter. A color scale was also used to map the variations of distance on the scapula

surface, with the red color denoting the zone of minimum distance and other colors denoting the areas of increased distance (Fig. 5).

Eventually, the following two criteria were applied: 1) Increased penetration depth results in increased soft tissue compression. Thus, when performed repetitively, the greater the penetration depth is, the more potentially damageable for the joint the internal impingement can be; 2) given the thickness of the potential impinged tissues, subacromial impingement was considered when the computed humero-acromial distance was < 6 mm, as suggested in previous studies [8, 19].

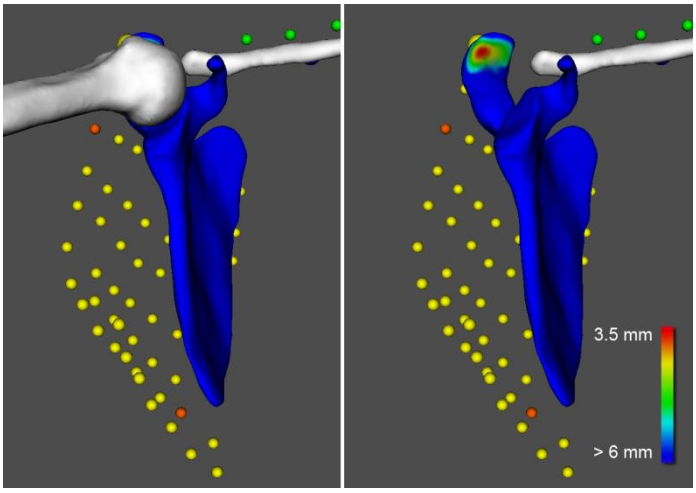

Fig. 5 Visualization of the humero-acromial distance during motion (anterior view). The colors represent the variations of distance between the acromion and humeral head. The red color denotes the zone of minimum distance. Note: the humerus is not shown in the second view for clarity.

2.6. Statistical analysis

A statistical analysis was conducted for the two variants of tennis serve. For internal impingement, we computed the frequency of impingement, the mean values and the standard deviations (SD) of the penetration depth, and we created histograms displaying the frequency of distribution of the zone of impingement. For subacromial impingement, we calculated the frequency of impingement and the mean and SD of the minimum humero-acromial distance.

For the radiological analysis, the prevalence of rotator cuff abnormalities, labral lesions and bony changes were calculated, as well as the frequency of distribution of the location of diagnosed labral lesions. Cohen's kappa coefficient (K) was calculated to assess the interobserver agreement regarding the image analysis. The statistical software package R, version 3.1.1 was employed.

3. Results

3.1. MRI findings

The K value for interobserver agreement of shoulder lesion evaluation on MRI arthrograms was 0.86, representing excellent agreement [9]. We found eleven rotator cuff lesions in six subjects (Table 1) – three interstitial of the supraspinatus, three partial articular supraspinatus tendon avulsions (PASTA), three partial articular infraspinatus tendon

avulsions and two articular of the subscapularis. All lesions were located on the articular side.

Distribution of labral lesions in the different positions around the glenoid (Table 2) showed more pronounced labral lesions at the posterosuperior and superior positions. There was no radiographic evidence of bony changes such as Bankart lesions or intra-osseous cysts.

Figure 6 shows two typical lesions found in the tennis players' shoulders: a PASTA lesion and a posterosuperior labral lesion (torn labrum).

Fig. 6 a) Coronal T2 weighted MR image with fat saturation showing a PASTA lesion (arrow) b) Coronal T1 weighted MR image with fat saturation showing a posterosuperior labral lesion (arrow).

3.2. Simulation findings

For the flat serve, internal impingement was observed in 76% of the tennis players' shoulders. The majority of the contacts (60%) was located in the posterosuperior position of the glenoid (Fig. 7). The mean penetration depths varied from 1.43 mm to 1.85 mm depending on the cartilage considered. For the kick serve, internal impingement occurred in 75% of the cases. The contacts were distributed between the posterosuperior (60%), superior (60%) and anterosuperior (30%) positions of the glenoid (Fig. 7). The computed penetration depths were of similar intensity (mean range: 1.53 – 1.90 mm). For both serves, the most intense penetration depths were obtained for the glenoid labrum, with peak values of 2.71 mm. Interestingly, when those contacts occurred, they were located in the posterosuperior region of the glenoid. Table 3 summarizes for the reader mean values and standard deviations of computed penetration depths by movement.

Subacromial impingement was detected during flat serve for 29% of the tennis players' shoulders. 10% were located in the anterior part of the acromion and 19% were located in the lateral part of the acromion. The mean ± SD of the minimum humero-acromial distance was 7.43 ± 3.12 mm. During kick serve, subacromial impingement was slightly more frequent (38% of the tennis players' shoulders), with 13% and 25% of the cases located respectively in the anterior and lateral parts of the acromion. The mean ± SD of the minimum humero-acromial distance was 6.88 ± 3.47 mm.

4. Discussion

In this study, we have presented a methodology to perform functional simulations of the shoulder joints in extreme and complex positions. To our knowledge, shoulder impingement

during tennis serve has never been dynamically evaluated. Using this patient-specific measurement technique, impingement was actively assessed and demonstrated in-vivo. The results of this study showed that the detected internal impingements were mostly located in the posterosuperior or superior quadrant of the glenoid, and that subacromial impingement was less frequent when serving. MRI revealed eleven rotator cuff lesions and more pronounced labral lesions at the posterosuperior and superior positions of the glenoid. All lesions were located in the articular side, suggesting an internal impingement as origin.

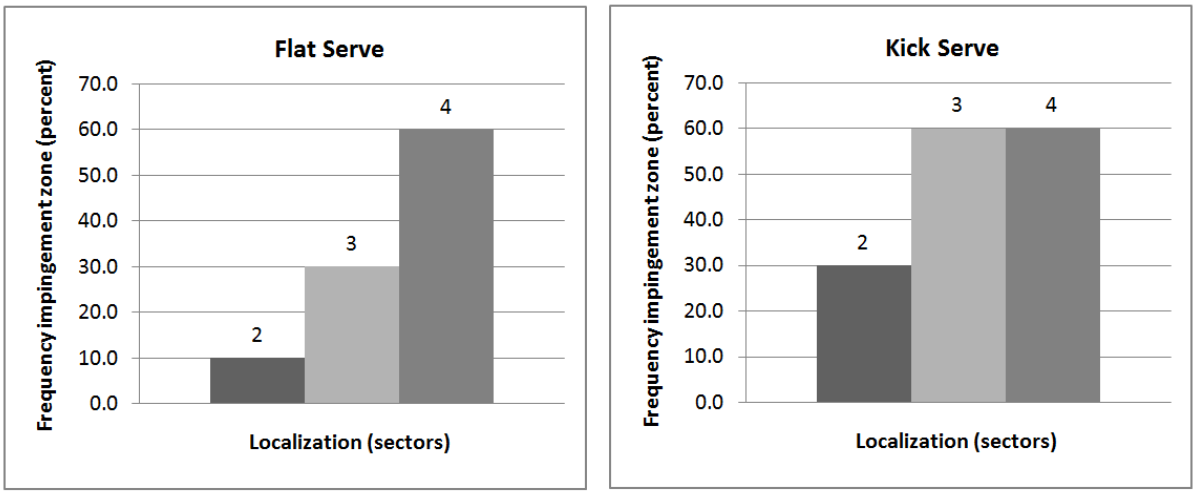

Fig. 7 Histograms showing the distribution of frequency of the computed internal impingement zones for each serve.

In the present study, nine of the ten tennis players presented radiographic signs of structural lesions that could be related to impingement syndrome due to overhead arm movements. However, the precise causes for these lesions remain unclear. Two main theories can be put forward. The first theory holds that repetitive contacts between the rotator cuff insertion and the posterosuperior glenoid rim – when the arm is placed in the cocked position of 90° abduction, full external rotation and extension [12] – may be responsible for rotator cuff tears and superior labral lesions [12, 23, 35]. The second theory holds that subacromial impingement may occur in overhead athletes because of narrowing of the subacromial space due to glenohumeral instability and/or muscle imbalance [15, 18, 27].

As shown by the results of this study, internal impingement was frequent when serving (75-76% of the tennis players' shoulders). For both tennis serves, the computed zones of impingement were mainly located in the posterosuperior or superior quadrant of the glenoid and this was relevant with respect to the MRI findings. Subacromial impingement remained low. We did not note shoulder instability in this population, as demonstrated in our previous study [7, 16]. Moreover, all subjects had a competent rotator cuff. The repetitive posterosuperior internal impingements seem thus to be the most plausible explanation for these lesions that are not always symptomatic, as previously observed [13].

The computed penetration depths varied from 1.43 to 1.90 mm in average for both tennis serves, with peak values of 2.71 mm for the labrum in posterosuperior position. Knowing that the glenoid labrum has superiorly and posteriorly an average height of 6-11 mm [3], the labrum is already compressed in our simulation during the late cocking stage of the serve – and this without accounting for the rotator cuff insertion that may also impinge between the greater tuberosity of the humeral head and the posterosuperior labrum. It is therefore most

likely that our results underestimated labral compressions. In fact, the true extent of compression cannot be determined without a more advanced simulation, taking into account the 3D shapes of the rotator cuff tendons and the soft tissues deformation under loads. Future work should hence include a 3D reconstruction of the rotator cuff from MRI data, as well as a physically-based simulation of the chondrolabral and tendon structures. A clinical trial could also be performed to validate the impingement estimates. Nevertheless, according to our data, there is little doubt that the glenohumeral articular surface is exposed to high mechanical stress.

There are potential limitations to the accuracy of the global set-up. Indeed, errors in our methodology could originate from the kinematics computation from motion capture data (translational error < 3 mm, rotational error < 4°). Since the measurements are external (no direct access to the joint), motion capture is generally subject to greater errors than other techniques (e.g., dynamic MRI, fluoroscopy). However, this modality is not harmful and allows the recording of large ranges of high velocity motion, such as tennis strokes. The second limitation of this study is the use of the humero-acromial distance to assess subacromial impingement, which does not take into account precise measurements of the thickness of the impinged soft tissues. Again, one improvement could be to perform a more advanced simulation accounting for the 3D shapes and movements of the rotator cuff tendons.

In summary, we conclude from our data that tennis players presented frequent radiographic signs of structural lesions which seem to be mainly related to posterosuperior internal impingement due to repetitive abnormal motion contacts. We believe that recurrent posterosuperior internal impingement could lead with time to cartilage/tendon hyper compression and therefore could be a potential factor of damages of the glenoid labrum and rotator cuff tendons.

This study[1] offers novel insights into the analysis of shoulder impingement that could, with future studies, be generalized to other shoulder pathologies and sports. This method[2] may open new horizons leading to improvement in impingement comprehension.

Acknowledgments

This work was supported by grants from La Tour Hospital, Geneva, Switzerland, and from the European Society for Surgery of the Shoulder and the Elbow (ESSSE).

Conflict of interest

The authors declare that they have no conflict of interest.

[1] This study won the *Best Technical Paper Award* at the 14th Annual Meeting of the International Society for Computer Assisted Orthopaedic Surgery (CAOS) in Milan, 2014.

[2] A video summarizing the method and complementary information about this work can be found at http://www.artanim.ch/Shoulder3D

References

1. Abrams G, Renstrom P, Safran M (2012) Epidemiology of musculoskeletal injury in the tennis player. Br J Sports Med 46:492–498

2. Bankart A (1923) Recurrent or habitual dislocation of the shoulder-joint. Br Med J 2(3285):1132–1133

3. Carey J, Small C, Pichora D (2000) In situ compressive properties of the glenoid labrum. J Biomed Mater Res 51(4):711–716

4. Charbonnier C, Assassi L, Volino P, Magnenat-Thalmann N (2009) Motion study of the hip joint in extreme postures. Vis Comput 25(9):873–882

5. Charbonnier C, Kolo F, Duthon V, Magnenat-Thalmann N, Becker C, Hoffmeyer P, Menetrey J (2011) Assessment of congruence and impingement of the hip joint in professional ballet dancers. Am J Sports Med 39(3):557–566

6. Charbonnier C, Chagué S, Kolo F, Chow J, Lädermann A (2014) A patient-specific measurement technique to model the kinematics of the glenohumeral joint. Orthop & Traumatol: Surg & Res 100(7):715-719

7. Charbonnier C, Chagué S, Kolo F, Lädermann A (2014) Analysis of shoulder impingement and stability in tennis players. In: Proc of the 13th International Symposium on 3D Analysis of Human Movement, Lausanne, Switzerland

8. Chopp J, Dickerson C (2012) Resolving the contributions of fatigue-induced migration and scapular reorientation on the subacromial space: An orthopaedic geometric simulation analysis. Hum Mov Sci 31:448–460

9. Cohen J (1960) A coefficient of agreement for nominal scales. Educ Psychol Meas 20:37–46

10. Cools A, Declercq G, Cagnie B, Cambier D, Witvrouw E (2008) Internal impingement in the tennis player: rehabilitation guidelines. Br J Sports Med 42:165–171

11. Creveaux T, Dumas R, Hautier C, Macé P, Chèze L, Rogowski I (2013) Joint kinetics to assess the influence of the racket on a tennis player's shoulder. J Sports Science Med 12:259–266

12. Davidson P, Elattrache N, Jobe C, Jobe F (1995) Rotator cuff and posterior-superior glenoid labrum injury associated with increased glenohumeral motion: a new site of impingement. Shoulder Elbow Surg 4(5):384–390

13. Girish G, Lobo L, Jacobson J, Morag Y, Miller B, Jamadar D (2011) Ultrasound of the shoulder: asymptomatic findings in men. AJR Am J Roentgenol 197:713-719

14. Graichen H, Hinterwimmer S, Eisenhart-Rothe R, Vogl T, Englmeier KH, Eckstein F (2005) Effect of abducting and adducting muscle acitivity on glenohumeral translation, scapular kinematics and subacromial space width in vivo. J Biomech 38(4):755–760

15. Hallstrom E, Karrholm J (2006) Shoulder kinematics in 25 patients with impingement and 12 controls. Clin Orthop Relat Res 448:22–27

16. Lädermann A, Chagué S, Kolo F, Charbonnier C (2014) Kinematics of the shoulder joints in tennis players. J Sci Med Sport, In Press

17. Leardini A, Chiari L, Croce UD, Cappozzo A (2005) Human movement analysis using stereophotogrammetry Part 3: Soft tissue artifact assessment and compensation. Gait & Posture 21:212–225

18. Ludewig P, Cook T (2002) Translations of the humerus in persons with shoulder impingement symptoms. J Orthop Sports Phys Ther 32(6):248–259

19. Maeseneer MD, Roy PV, Shahabpour M (2006) Normal mr imaging anatomy of the rotator cuff tendons, glenoid fossa, labrum, and ligaments of the shoulder. Radiol Clin N Am 44:479–487

20. Manske R, Grant-Nierman M, Lucas B (2013) Shoulder posterior internal impingement in the overhead athlete. Int J Sports Phys Ther 8(2):194–204

21. Massimini D, Boyer P, Papannagari R, Gill T, Warner J, Li G (2012) In-vivo glenohumeral translation and ligament elongation during abduction and abduction with internal and external rotation. J Orthop Surg Res 7:29–38

22. Matsuki K, Matsuki K, Yamaguchi S, Ochiai N, Sasho T, Sugaya H, Toyone T, Wada Y, Takahashi K, Banks S (2012) Dynamic in vivo glenohumeral kinematics during scapular plane abduction in healthy shoulders. J Orthop Sports Phys Ther 42(2):96–104

23. Meister K (2000) Internal impingement in the shoulder of the overhand athlete: pathophysiology, diagnosis, and treatment. Am J Orthop 29(6):433–438

24. Meister K, Andrews J, Batts J, Wilk K, Baumgarten T (1999) Symptomatic thrower's exostosis. arthroscopic evaluation and treatment. Am J Sports Med 27(2):133–136

25. Neer C (1972) Anterior acromioplasty for chronic impingement syndrome in the shoulder: a preliminary report. J Bone Joint Surg Am 54:41–50

26. Nyffeler R, Werner C, Sukthankar A, Schmid M, Gerber C (2006) Association of a large lateral extension of the acromion with rotator cuff tears. J Bone Joint Surg Am 88(4):800–805

27. Page P (2011) Shoulder muscle imbalance and subacromial impingement syndrome in overhead athlete. Int J Sports Phys Ther 6(1):51–58

28. Reid M, Elliott B, Alderson J (2007) Shoulder joint loaload in the hhigh performance flat and kick tennis serves. Br J Sports Med 41:884–889

29. Roux E, Bouilland S, Godillon-Maquinghen AP, Bouttens D (2002) Evaluation of the global optimisation method within the upper limb kinematics analysis. J Biomech 35:1279–1283

30. Sakurai S, Reid M, Elliott B (2013) Ball spin in the tennis serve: spin rate and axis of rotation. Sports Biomech 12(1):23–29

31. Salvia P, Jan SVS, Crouan A, Vanderkerken L, Moiseev F, Sholukha V, Mahieu C, Snoeck O, Rooze M (2009) Precision of shoulder anatomical landmark calibration by two approaches: A CAST-like protocol and a new anatomical palpator method. Gait & Posture 29(4):587–591

32. Schneider P, Eberly D (2003) Geometric Tools for Computer Graphics. The Morgan Kaufmann Series in Computer Graphics and Geometric Modeling

33. Snyder S, Pachelli A, Pizzo WD, Friedman M, Ferkel R, Pattee G (1991) Partial thickness rotator cuff tears: results of arthroscopic treatment. Arthroscopy 7(1):1–7

34. Timmons M, Lopes-Albers AD, Borgsmiller L, Zirker C, Ericksen J, Michener L (2013) Differences in scapular orientation, subacromial space and shoulder pain between the full can and empty can tests. Clin Biomech 28:395–401

35. Walch G, Boileau P, Noel E, Donell S (1992) Impingement of the deep surface of the supraspinatus tendon on the posterior glenoid rim: an arthroscopic study. J Shoulder Elbow Surg 1:238–245

36. Waldt S, Burkart A, Imhoff A, Bruegel M, Rummeny E, Woertler K (2005) Anterior shoulder instability: accuracy of mr arthrography in the classification of anteroinferior labroligamentous injuries. Radiology 237(2):578–583

37. Warner M, Chappell P, Stokes M (2012) Measuring scapular kinematics during arm lowering using the acromion marker cluster. Hum Mov Sci 31:386–396

38. Whiteside D, Elliott B, Lay B, Reid M (2014) The effect of racquet swing weight on serve kinematics in elite adolescent female tennis players. J Science Med Sport 17(1):124–128

39. Wong F, Keung J, Lau N, Ng D, Chung J, Chow D (2014) Effects of body mass index and full body kinematics on tennis serve speed. J Hum Kinet 40:21–28

40. Wu G, van der Helm F, Veegerc H, Makhsouse M, Royf PV, Angling C, Nagelsh J, Kardunai A, McQuadej K, Wangk X, Wernerl F, Buchholzm B (2005) ISB recommendation on definitions of joint coordinate systems of various joints for the reporting of human joint motion - part II: shoulder, elbow, wrist and hand. J Biomech 38:981–992

Table 1 Rotator cuff lesions

	Rotator cuff condition in tennis players (*n* = 10)*				
Position	**Normal**	**Partial articular**	**Partial bursal**	**Interstitial**	**Complete**
Supraspinatus	5	3	0	3	0
Infraspinatus	7	3	0	0	0
Subscapularis	8	2	0	0	0
Teres minor	10	0	0	0	0
Total lesions		8	0	3	0

*Data are the number of subjects.

Table 2 Labral lesions

	Labrum condition in tennis players (*n* = 10)*				
Position	**Normal**	**Degeneration**	**Tear**	**Detachment**	**Ossification**
Anterior	10	0	0	0	0
Superior	7	0	3	0	0
Posterosuperior	7	2	2	0	0
Posterior	8	2	0	0	0
Posteroinferior	10	0	0	0	0
Inferior	8	0	0	2	0
Anteroinferior	10	0	0	0	0
Total lesions		4	5	2	0

*Data are the number of subjects.

Table 3 Computed penetration depths (mm) by movement (*n* = 30)*

Movements	Humeral cartilage Mean ± SD (range)	Glenoid cartilage Mean ± SD (range)	Glenoid labrum Mean ± SD (range)
Flat serve	1.18 ± 0.25 (0.79 – 1.61)	1.43 ± 1.30 (0.79 – 1.76)	1.85 ± 0.48 (1.12 – 2.71)
Kick serve	1.23 ± 0.20 (1.05 – 1.62)	1.53 ± 0.24 (1.08 – 1.87)	1.90 ± 0.34 (1.65 – 2.71)

*Data are the number of trials (3 trials per subject)